Observation of Fine Structure in Bicontinuous Phase-Separated Domains of a Polymer Blend by Laser Scanning Confocal Microscopy

Hiroshi Jinnai,*,†,‡ Hiroshi Yoshida,†,§ Kohtaro Kimishima,†,∥ Yoshinori Funaki,†,⊥ Yoshitsugu Hirokawa,†,# Alexander E. Ribbe,†,& and Takeji Hashimoto*,†,○

Hashimoto Polymer Phasing Project, ERATO, Japan Science and Technology Corporation; and Department of Polymer Chemistry, Graduate School of Engineering, Kyoto University, Kyoto 606-8501, Japan

Received February 1, 2001

ABSTRACT: Laser scanning confocal micrographs for blends of poly(styrene-*ran*-butadiene) (SBR) and polybutadiene (PB) demonstrated the existence of fine structures inside one of the well-characterized macroscopically phase-separated bicontinuous domains, in the depth range of the blends belonging to the bulk. The average size of the fine structures was on the submicrometer length scale, while the characteristic spacing of the macroscopically phase-separated domains was on the order of 10 μm. Fluorescence laser scanning confocal micrographs revealed that the fine structures exist only in the SBR-rich phase. Although the driving force for the formation of the fine structures needs to be investigated further, a small amount of PB molecules in the SBR-rich domains seems to play an important role. Illumination and highlights were shed on the advantage of using laser scanning confocal microscopy for investigation of fine structures in the polymer blends.

I. Introduction

The dynamics and pattern formation of polymer blends undergoing spinodal decomposition (SD) have been the subject of both theoretical and experimental investigations, providing a fascinating example of nonlinear nonequilibrium phenomena.[1−3] Over the last 2 decades, scattering studies employing light[4−8] and neutrons[9−13] have been used to investigate the growth of concentration fluctuations via SD. The characteristic morphology of the SD process, a bicontinuous domain structure, and its growth have already been satisfactorily understood, at least from a global and statistical point of view.

On the other hand, experiments based on real-space analysis employing light or electron microscopy have so far provided only limited pieces of information, although they may be expected to offer further insights into the local structures of the phase-separated polymer blends. One of the major drawbacks of conventional light microscopy is its limited resolution both in lateral (parallel to the focal plane) and axial (perpendicular to the focal plane) directions. In most cases, images obtained from conventional optical microscopy are smeared due to its fairly large focal depth, which makes them inappropriate for quantitative analysis. Transmission electron microscopy has sufficient resolution, but it is often very difficult to selectively stain the sample to obtain the required contrast.

To overcome these problems, laser scanning confocal microscopy (LSCM) has recently been applied to polymer blends.[14−19] LSCM excludes out-of-focus information by focusing through a small aperture (a confocal pinhole).[20−23] This feature ensures that information in the image arrives only from a particular depth of the specimen, hence providing a method to observe an optically sliced section of the object in the specimen. The optical sections thus obtained can be reconstructed into a three-dimensional (3D) image by an image processing. We have previously demonstrated that LSCM is an excellent tool for studying the phase-separated structures of a polymer blend.[17−19] The 3D images determined by LSCM observations were shown to be capable of quantitatively capturing the bicontinuous domain structure,[17] and we have succeeded in determining local interfacial curvatures and their distribution in the bicontinuous structure.[18,19]

As pointed out in our previous communication,[17] the bright phase observed in the reflection LSCM images of a mixture of poly(styrene-*ran*-butadiene) (SBR) and polybutadiene (PB) appeared to consist of dotlike structures (see Figure 1 of ref 17). In the present report we confirm the existence of the fine structures by carefully considering the resolution of LSCM. Identification of the bright phase observed in the reflection LSCM image, which was less clear in the previous study,[17] was achieved by an additionally employed fluorescence LSCM technique, using a mixture of SBR and anthracene-labeled polybutadiene (PB−AN).

II. Experimental Section

PB's, SBR's and a poly(deuterated butadiene) (dPB) were synthesized by the following standard anionic polymerization methods. PB−AN's were prepared by the reaction of 9-anthryldiazomethane with PB's containing carboxyl groups,

* To whom correspondence should be addressed.
† Japan Science and Technology Corporation.
‡ Present address: Department of Polymer Science and Engineering, Kyoto Institute of Technology, Matsugasaki, Kyoto 606−8585, Japan.
§ Present address: Department of Electronic Materials Research, Hitachi Research Laboratory, Hitachi, Ltd., Hitachi, Ibarakia 319-1292, Japan.
∥ Present address: Research & Development Center, Tonen Chemical Corp., 3−1 Chidori, Kawasaki-ku, Kawasaki 210−0865, Japan.
⊥ Present address: Research Center, Daicel Industries Ltd., 1239 Shinzaike, Aboshi-ku, Himeji, Hyogo 671-1283 Japan.
Present address: Zeon Corporation, Research & Development Center, 1−2−1 Yako, Kawasaki-shi, Kanagawa 210−9507, Japan.
& Present address: Department of Chemistry, Purdue University, 1393 Brown Bldg. Box 193 West Lafayette, IN 47906.
○ Kyoto University.

10.1021/ma010190d CCC: $20.00
Published on Web 06/22/2001

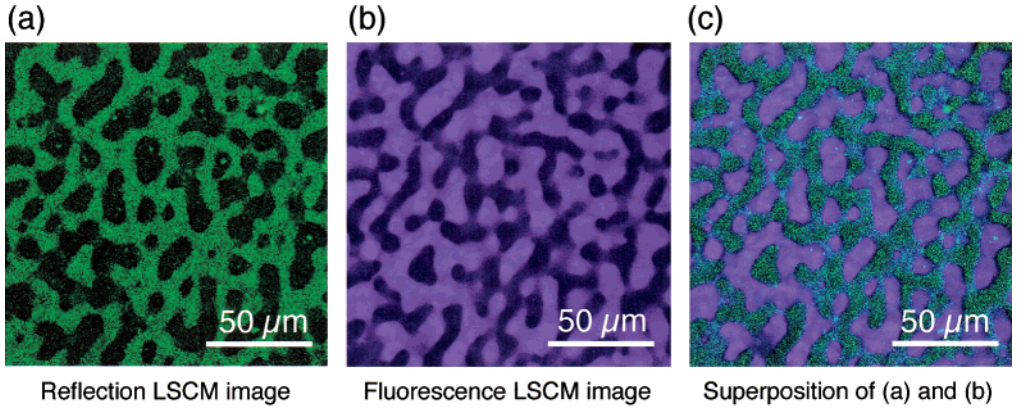

Figure 1. LSCM images at depth ca. 20 μm from the sample surface of the SBR/PB−AN mixture (50/50 wt/wt %) first phase-separated at 100 °C for ca. 44 h, then cooled to and observed at 23 °C. (a) Reflection LSCM image observed with $\lambda = 0.488$ μm and 40×/1.3 objective. $d_{lateral} = 0.23$ μm and $d_{axial} = 0.97$ μm, respectively, under this configuration of LSCM. (b) Fluorescence LSCM image of the same field as in image (a) observed using $\lambda = 0.364$ μm and 40×/1.3 objective. $d_{lateral} = 0.17$ μm and $d_{axial} = 1.57$ μm, respectively, under this configuration of LSCM. (c) Superposition of the two images, a and b, which are shown in green and purple, respectively. The number-averaged molecular weights and their distributions of the SBR and PB−AN used are as follows: SBR, M_n 14.8 × 10^4 ($M_w/M_n = 1.21$); PB−AN, M_n 5.7 × 10^4 ($M_w/M_n = 1.56$).

which had been introduced by the 1,3-dipole addition of *p*-carboxybenzhydroxamylchrolide in the presence of triethylamine.[24] The average number of anthryl groups introduced into a single polymer chain was 2−4.

The SBR/PB blends were prepared as follows. The mixtures of SBR and PB were dissolved in toluene as solutions of approximately 5−7 wt % total polymer concentration. The homogeneous solutions were then cast into thin films, which were subsequently dried in a vacuum oven at room temperature. The SBR/PB blends have an upper critical solution temperature (UCST) type phase diagram.[25] The cloud points of the mixtures investigated in this work could not be found in the experimental temperature range (25−100 °C). Thus, the sample films obtained were in the two-phase region and appeared to be translucent due to phase separation. The phase-separated films were homogenized by mechanical mixing using Baker's transformation[26] and placed between two coverslips with a Teflon sheet (thickness: 200 μm) used as a spacer. The samples were then heat-treated for 44 h at 100 °C for phase separation via SD and quenched to room temperature for the LSCM observations described below, unless otherwise stated. The SBR/PB−AN and dPB/PB−AN blends were prepared following the similar procedure described above.

The LSCM observations of the films were performed using an LSM410 (Carl-Zeiss, Jena, Germany) with a 100× objective (numerical aperture (*N. A.*) = 1.40, Plan-Apochromat 100×/1.4 oil, Carl-Zeiss) or 40× objectives (*N. A.* = 1.30, Plan-Apochromat 40×/1.3 oil, Carl-Zeiss) at room temperature (23 °C). In the present study, the LSCM was operated both as a reflection and as a fluorescence confocal microscope. For the former, an Ar laser having a wavelength (λ) of 0.488 μm was used as a light source. For the latter, an Ar laser with $\lambda = 0.364$ μm was used to excite the anthryl groups attached to PB chains, and the fluorescence emitted from the dye molecules was selectively detected by a combination of a dichromatic mirror and a band-pass filter (which transmits the light components with wavelength between 295 and 440 nm) in front of the detector. LSCM is particularly attractive because of its enhanced resolutions both in lateral and axial directions. The lateral and axial resolutions of the reflection LSCM using the 100×/1.40 objective with $\lambda = 0.488$ μm were $d_{lateral} = 0.16$ μm [27] and $d_{axial} = 0.54$ μm,[28] respectively. The axial resolution of the fluorescent LSCM using the same objective but $\lambda = 0.364$ μm was $d_{axial} = 0.75$ μm. All optical slices were at least 20 μm distant from the coverslips, to avoid possible surface effects on the phase-separated structures.

III. Results and Discussion

Figure 1a shows a reflection LSCM image of the SBR/PB−AN blend phase-separated at 100 °C for ca. 44 h. The green part of the image is one of the phase-separated bicontinuous domains developed via the SD process.[17,18] The mean spacing between the domains is estimated to be 8 μm, which is much larger than $d_{lateral} = 0.23$ μm and $d_{axial} = 0.69$ μm. To identify whether the SBR-rich phase shows up as the green bright regions or dark regions in Figure 1a, a fluorescence LSCM image was taken at exactly the same field for the same sample, as shown in Figure 1b. The bright purple regions in the micrograph reveal the existence of the anthracene-labeled polybutadiene phase. Figure 1c represents a superposed image of the reflection image (Figure 1a) and the fluorescence image (Figure 1b). The two images are found to be complementary to each other. We therefore conclude that the bright regions and the dark regions of the micrograph obtained by the reflection LSCM (Figure 1a) correspond to the SBR-rich domains and the PB-rich domains, respectively.

The contrast in the reflection image shown in Figure 1a may be associated with a difference in refractive indices of the two components.[30] If the SBR-rich regions in the sample were homogeneous, they should have appeared dark under the LSCM observation and only a part of the interface between the SBR-rich domains and PB-rich domains which satisfies a high reflectivity should have appeared bright. Before going into more detailed discussion of Figure 1a, we will present another datum in Figure 2 to help further interpretation of Figure 1a.

Parts a and b of Figure 2 display reflection and fluorescence LSCM images of a phase-separated polymer blend of dPB and PB−AN, respectively, in the late stage SD process just as in the case of SBR/PB−AN. The bright purple regions in the fluorescent image in Figure 2b are the PB−AN-rich domains. As can be seen from Figure 2, parts a−c, all together, only the interfacial region of the domains appeared bright and interior parts of both the dPB-rich and PB−AN-rich domains were dark under the reflection mode (Figure 2a) as expected.[31] On the other hand, as seen in Figure 1a, the SBR-rich domains in the SBR/PB polymer blend appeared uniformly bright, although they seem to consist of dotlike small objects. This result suggests that the SBR-rich phase in the SBR/PB blend contains

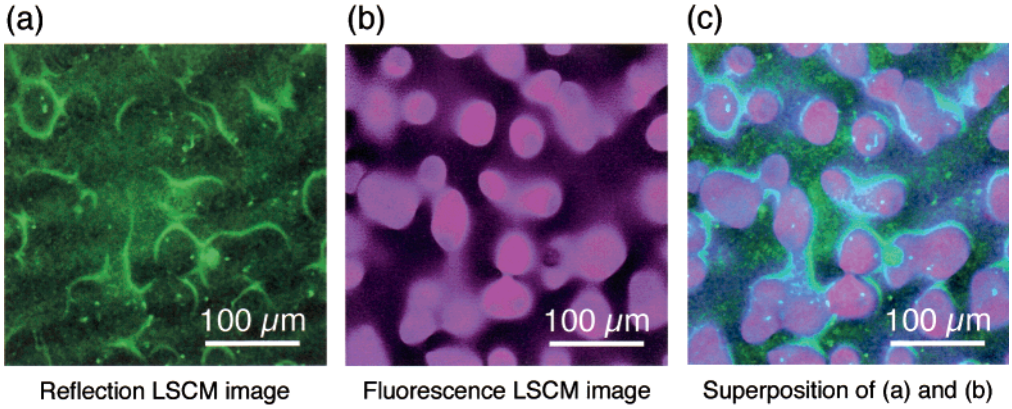

Figure 2. LSCM images of dPB/PB−AN blend (50/50 wt/wt %) first phase-separated at 40 °C for 164 h and then observed at 23 °C. (a) Reflection LSCM image observed with $\lambda = 0.488\ \mu$m and 40×/1.3 objective. $d_{lateral} = 0.23\ \mu$m and $d_{axial} = 1.0\ \mu$m, respectively, under this configuration of LSCM. (b) Fluorescence LSCM image of the same field as image (a) observed using $\lambda = 0.364\ \mu$m for excitation of the labels and 40×/1.3 objective. $d_{lateral} = 0.17\ \mu$m and $d_{axial} = 1.35\ \mu$m, respectively, under this configuration of LSCM. (c) Superposition of the two images, a and b, which are shown in green and purple, respectively. The number-averaged molecular weights and their distributions of the dPB and PB−AN used are as follows: dPB, $M_n = 12.8 \times 10^4$ ($M_w/M_n = 1.12$); PB−AN, $M_n = 8.9 \times 10^4$ ($M_w/M_n = 1.07$).

inhomogeneity in refractive index on the submicrometer length scale.

It is very important to note that this inhomogeneity is not present in either the PB-rich phase in the SBR/PB blend or in both of the phase-separated domains of the dPB/PB−AN blend. The lack of the inhomogeneities in the PB-rich domain in the SBR/PB blends clearly rules out the possibility that the inhomogeneities are an artifact brought by a special protocol related to an incompleteness of the mechanical homogenization process. If this is the case, the inhomegeneities could have been seen in the PB-rich phase as well. The inhomogeniety in SBR-rich domains give rise to scattering, and this scattering is believed to cause a bright contrast under the reflection LSCM mode (scattering-induced contrast generation).[30] This scattering-induced contrast generation in the reflection LSCM was unequivocally confirmed in this work by a combined use of the reflection and fluorescence LSCM technique, which is one of the important conclusions of this paper. In Figure 1a, we notice some small bright domains in the dark PB phase. These are expected to be the SBR domains generated during the coarsening processes via a breakup of the percolated SBR domains.

A typical reflection LSCM image obtained for the SBR/PB blends using the 100× objective, thus having a higher resolution than Figure 1a, is shown in Figure 3. The mixture was phase-separated at 100 °C for ca. 40 h after the mechanical homogenization. As confirmed in the discussion in conjunction with Figure 1, the bright areas in Figure 3 are the SBR-rich domains. The expanded and digitally enhanced[32] image of the region shown by the white rectangle in Figure 3a is presented in Figure 3b. As predicted, the SBR-rich domains did not appear homogeneous but consisted of small bright objects.[33] The small-scale objects observed in Figure 3b have a characteristic size of approximately 0.6 μm, which is larger than the resolution limit ($d_{lateral} = 0.16\ \mu$m) of the 100×/1.40 objective, ruling out the possibility that these objects are optical illusions. To our knowledge, the presence of such inhomogeneity on the fine length scale inside phase-separated bicontinuous domains has not been reported.[34]

The inhomogeneity in refractive indices in the SBR-rich domains can be either (i) dynamical composition fluctuations (dynamical inhomogeneity) or (ii) static

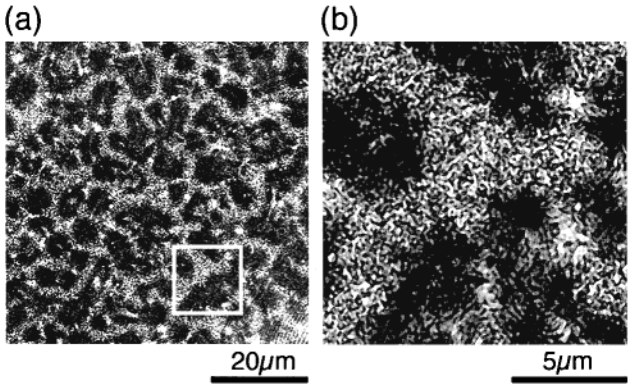

Figure 3. Reflection LSCM images of SBR/PB blend (50/50 wt/wt %) first phase-separated at 100 °C for ca. 145 h and then observed at 23 °C. The observations were performed using $\lambda = 0.488\ \mu$m and 100×/1.4 objective. Image b is a magnified image of the white rectangular region in image a. To make the fine structure clearer, in image b, two kinds of digital image filters were successively applied to the original image a. In the first place, a median filter with a 5 × 5 matrix was used to get rid of random noise without smoothing edges in the image. Subsequently, a high-pass filter with a 5 × 5 matrix was utilized to enhance the edges of the fine structure.[39] The number-averaged molecular weights and their distributions of the SBR and PB used are as follows: SBR, $M_n = 14.8 \times 10^4$ ($M_w/M_n = 1.21$); PB, $M_n = 17.2 \times 10^4$ ($M_w/M_n = 1.30$).

composition fluctuations (fixed inhomogeneity). As for the former possibility (point i), we may further think about the following two cases. The present specimen was subjected to a heat-treatment at 100 °C in order to develop phase-separated structure in the late stage SD and then to quenching to 23 °C for observation with LSCM. The observation temperature of 23 °C is still higher than glass transition temperatures of both PB-rich and SBR-rich phases, and thus the **dynamical composition fluctuations** within the phase-separated SBR-rich domains may exist even at 23 °C (to be designated as **(**i-a**)**) as well as at 100 °C. In this case the fluctuations at 23 °C are enhanced compared with those at 100 °C. There is another possibility (to be designated as **(**i-b**)**) that phase separation of PB and SBR may occur inside the SBR-rich domains when the temperature decreases from 100 to 23 °C. This is because the SBR-rich domains at 100 °C may contain a small amount of PB and become metastable or unstable

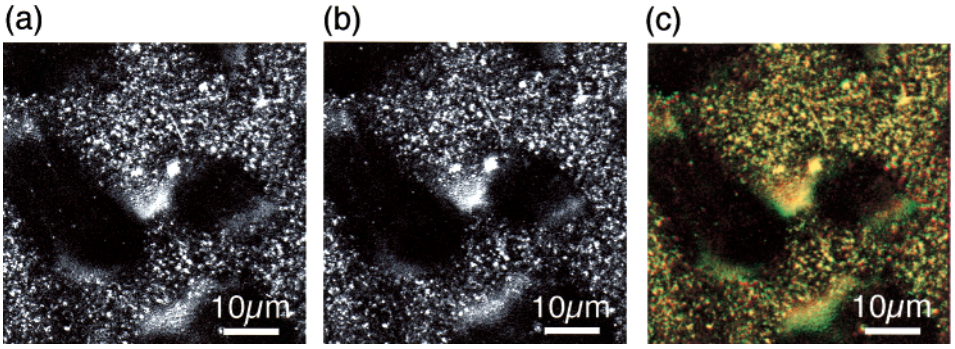

Figure 4. Reflection LSCM images of SBR/PB−AN blend (50/50 wt/wt %) first phase-separated at 30 °C for 26 h and then observed at 23 °C. The observations were performed using $\lambda = 0.488$ μm and 100×/1.4 objective. Image b was taken 25 min after the observation of image a at the same view field. Image c shows a superposition of images a and b, displayed in green and red, respectively. The number-averaged molecular weights and their distributions of the SBR and PB−AN used are as follows: SBR, $M_n = 8.0 \times 10^4$ ($M_w/M_n = 1.03$); PB−AN, $M_n = 7.6 \times 10^4$ ($M_w/M_n = 1.02$).

upon cooling, giving rise to a phase-separated structure (**two-step phase separation**[35]). If this is the case, the heterogeneities inside the SBR-rich domains reflect a snapshot of the second-step phase separation and should grow with time, no matter how slow it might be. However, this is not what we observed experimentally. Before going into detailed discussion about the fixed inhomogeneity (ii), we shall first discuss the scenarios for the dynamical inhomogeneity (i-a) and (i-b) in detail below.

As for the former possibility (i), further reflection LSCM observations presented below in Figure 4 suggest that the fine objects observed in the SBR-rich domains might not be due to a snapshot of the dynamical thermal fluctuations (i-a). Figure 4 presents LSCM images of SBR/PB−AN blend film phase-separated deliberately at 30 °C (not at 100 °C) for 26 h after the mechanical homogeneization and observed at 23 °C. Parts a and b of Figure 4 were taken at a fixed view field at time interval of 25 min but each image, a or b itself, was captured in 30 s. Although the phase-separation temperature and observation temperature is almost same, the fine objects still exist in the SBR-rich domains which appear to be bright. Figure 4c shows an image of Figure 4, parts a and b, which are respectively displayed in green and red and then, superimposed on each other. This image clearly shows that the fine objects presented in Figure 4a exist in almost an identical configuration even after 25 min. Therefore, it is highly plausible to conclude that the fine objects observed by reflection LSCM in Figure 4 are not a snapshot of the dynamical thermal composition fluctuations (i-a). The results obtained in Figure 4 also imply that the fine objects observed in Figure 3 by reflection LSCM may not be necessarily due to effects of the two-step phase separation (i-b), simply because the fine objects are observed even in Figure 4 which was taken at the observation temperature (23 °C) close enough to the phase-separation temperature (30 °C). If the fine structures are formed as a consequence of the two-step phase separation, the fine structures should grow into larger objects and be eventually segregated out from the SBR-rich domains into the PB−AN-rich domains.[35] This is not the case here. In any case, the fine objects appear to be due to the static one (ii) rather than the dynamical one (i).

Let us next examine possible origins of the fine structure from the static inhomogeneity (ii). The SBR's used in the present study were polymerized by anionic polymerization. It has been reported that anionically polymerized SBR has a sequence distribution of styrene and butadiene units different from that of radically polymerized SBR:[36] the former had longer sequences (ca. 35 units) of styrene units than the latter. Namely, the SBR we used could have some block character in the distribution of the styrene and the butadiene units, which has to be taken into consideration.[37] There is a possibility (denoted **(**ii-a**)**) that **an association of the styrene sequences of the SBR chains inside the SBR-rich phase** might account for the origin of the fine structure inside the SBR-rich domains. To test this effect (ii-a), we heat-treated virgin SBR specimens under the same experimental conditions as the SBR/PB mixtures. However, even after 4 days of the thermal treatment, including occasional intermittent observations, there appeared to be no evidence for the presence of fine structure in the pure SBR sample under reflection LSCM. This experimental result indicates that the existence of a sequence distribution in SBR alone could not explain the formation of the fine structures in the SBR-rich domains but that PB chains exist in the SBR-rich phase may play an important role.

The fine structure (Figure 3b) appears to be quite similar to the bicontinuous structure that can be seen in Figure 1. They appeared to be interconnected to one another in a similar way to the bicontinuous structure formed by the SBR-rich and PB-rich domains, although the former appear to be more random than the latter. Laurer et al.[38] have reported a channel-like structure, which is similar to the present fine structure, exists in one of the domains of polymer blend systems. Their blends were composed of homopolystyrene and poly(styrene-*ran*-isoprene)-*block*-poly(styrene-*ran*-isoprene) block copolymer ((75/25)-*block*-(50/50)). They found that at low homopolystyrene fractions, the styrene and isoprene block sequences in the block copolymer induce competition between attractive and repulsive interactions with the homopolystyrene chains, resulting in the formation of thin homopolystyrene channel structures in a disordered random block copolymer matrix. We suppose that a similar kind of competitive segmental interaction may exist between styrene and butadiene sequences in the SBR and a small amount of PB chains in the SBR-rich domains, which may stabilize the channels (or the microphase) composed of associating PB chains in the SBR matrix as a consequence of an emulsifying effect of SBR for the PB chains. This **weak microphase separation of the PB chains** enhanced by the emulsifying effects of SBR seems to be the most plausible model (denoted **(**ii-b**)**) to account for the origin of the static inhomogeneity. If this is the

case, a mixture composed of SBR and PB with an appropriate blend composition should exhibit a similar fine structure, a confirmation of which is, however, left for future work.

IV. Concluding Remarks

The phase-separated structures developed via spinodal decomposition in a mixture of SBR and PB were investigated under laser scanning confocal microscopy. By combining the reflection and fluorescence LSCM images, we have clearly revealed that fine structures exist only in the SBR-rich phase. This fine structure is on the sub-microscopic length scale and seems to be bicontinuous. We elucidated that a small amount of PB molecules in SBR-rich domains definitely play an important role.

We further discussed four possible models: (i-a) and (i-b) based on the dynamical inhomogeneities and (ii-a) and (ii-b) based on the static heterogeneities. We suggested model (ii-b), the channels composed of associating PB chains in the SBR matrix assisted by an emulsifying effect of SBR, as a most plausible model. We hope the present study may act as a catalyst for further discussion and experiments, especially with a better controlled system (having a phase diagram in the experimentally easily accessible temperature range) and with a better defined thermal protocol.

Acknowledgment. We thank Japan Synthetic Rubber, Co. for their kind donation of some of the polymers used in the present study. H.J. is partially supported by the Japan Society of Promotion of Science (Grant-in-Aid for Scientific Research, No. 12750799).

References and Notes

(1) Gunton, J. D.; San Miguel, M.; Sahni, P. S. In *Phase Transitions and Critical Phenomena*; Domb, C., Lebowitz, J. L., Eds.; Academic Press: New York, 1983; p 269.
(2) Binder, K. In *Materials Science and Technology, Vol. 5, Phase Transformation in Materials*; Haasen, P., Vol. Ed; VCH: Weinheim, Germany, 1991.
(3) Hashimoto, T. *Phase Transitions* **1988**, *12*, 47. Hashimoto, T. In *Materials Science and Technology, Vol 12, Structure and Properties of Polymers*, Thomas, E. L., Vol. Ed; VCH: Weinheim, Germany, 1993.
(4) Hashimoto, T.; Itakura, M.; Hasegawa, H. *J. Chem. Phys.* **1986**, *85*, 6118. Hashimoto, T.; Itakura, M.; Shimidzu, N. *J. Chem. Phys.* **1986**, *85*, 6773.
(5) Okada, M.; Han, C. C. *J. Chem. Phys.* **1986**, *85*, 5317. Sato, T.; Han, C. C. *J. Chem. Phys.* **1988**, *88*, 2057.
(6) Hashimoto, T.; Takenaka, T.; Jinnai, H. *J. Appl. Crystallogr.* **1991**, *24*, 457.
(7) Takenaka, M.; Hashimoto, T. *J. Chem. Phys.* **1992**, *96*, 6177.
(8) Bates, F. S.; Wiltzius, P. *J. Chem. Phys.* **1989**, *91*, 3258.
(9) Higgins, J. S.; Fruitwala, H.; Tomlins, P. E. *Br. Polym. J.* **1989**, *21*, 247.
(10) Jinnai, H.; Hasegawa, H.; Hashimoto, T.; Han, C. C. *Macromolecules* **1991**, *24*, 282.
(11) Jinnai, H.; Hasegawa, H.; Hashimoto, T.; Han. C. C. *J. Chem. Phys.* **1993**, *99*, 4845. Jinnai, H.; Hasegawa, H.; Hashimoto, T.; Han. C. C. *J. Chem. Phys.* **1993**, *99*, 8154.
(12) Schwahn, D.; Hahn, K.; Springer, T. *J. Chem. Phys.* **1990**, *93*, 8383. Schwahn, D.; Janssen, S.; Springer, T. *J. Chem. Phys.* **1992**, *97*, 8775.
(13) Hashimoto, T.; Jinnai, H.; Hasegawa, H.; Han, C. C. *Physica A* **1994**, *204*, 261.
(14) Verhoogt, H.; van Dam, J.; Posthuma de Boer, A.; Draaijer, A.; Houpt, P. M. *Polymer* **1993**, *34*, 1325.
(15) Li, L.; Sosnowski, S.; Chaffey, C. E.; Balke, S. T.; Winnik, M. A. *Langmuir* **1994**, *10*, 2495.
(16) White, W. R.; Wiltzius, P. *Phys. Rev. Lett.* **1995**, *75*, 3012.
(17) Jinnai, H.; Nishikawa, Y.; Koga, T.; Hashimoto, T. *Macromolecules* **1995**, *28*, 4782.
(18) Jinnai, H.; Koga, T.; Nishikawa, Y.; Hashimoto, T.; Hyde, S. T. *Phys. Rev. Lett.* **1997**, *78*, 2248. Jinnai, H.; Nishikawa, Y.; Hashimoto, T. *Phys. Rev. E* **1999**, *59*, R2554.
(19) Nishikawa, Y.; Jinnai, H.; Koga, T.; Hashimoto, T. *Langmuir* **1998**, *14*, 1242.
(20) Wilson, T. In *Handbook of Biological Confocal Microscopy*, 2nd ed.; Pawley, J. B., Ed.; Plenum Publishing Corp.: New York, 1995; Chapter 11.
(21) Inoue, S. In *Handbook of Biological Confocal Microscopy*, 2nd ed.; Pawley, J. B., Ed.; Plenum Publishing Corp.: New York, 1995; Chapter 1.
(22) Wilson, T. In *Confocal Microscopy*; Willson, T., Ed.; Academic Press: London, 1990; Chapter 3.
(23) Wilson, T.; Carlini, A. R. *Opt. Lett.* **1987**, *12*, 227.
(24) Huigen, R. Angrew. *Chem. Int. Ed. Engl.* **1963**, *2*, 565.
(25) Izumitani, T.; Hashimoto, T. *J. Chem. Phys.* **l985**, *83*, 3694.
(26) Hashimoto, T.; Izumitani, T.; Takenaka, M. *Macromolecules* **1989**, *22*, 2293. Ribbe, A.; Hashimoto, T. *Macromolecules* **2000**, *33*, 7827.
(27) Actual resolution of LSCM should be carefully considered, because it depends strongly on the size of the confocal pinhole[23] and on the alignment of the optics. In the present report we have estimated d_{lateral} as follows. The resolution of a light microscope is defined as the full width at half-maximum (fwhm) of the intensity profile of an image of a point object.[21,22] We measured the intensity profile of the reflection LSCM image of an oil-immersed single latex sphere (diameter: 0.090 μm) using an Ar laser ($\lambda = 0.488$ μm) and the 100×/1.4 oil immersion objective. In the observation, diameter of the image of the confocal pinhole in the object plane was adjusted to 0.070 μm as suggested by Wilson.[20,22,23] The fwhm of a circular averaged profile of the latex sphere image, thus d_{lateral} of the microscope operated in the reflection mode using the 100×/1.4 oil immersion objective, was determined to be 0.16 μm.
(28) The axial resolution (d_{axial}) was considered as follows. It has been reported that the following equation gives an excellent fit to d_{axial} for reflection LSCM in the nearly aberration-free situation,[29]

$$d_{\text{axial}} = \left(1.41\frac{\lambda_{\text{em}}}{\lambda_{\text{exc}}}\right)\left\{\frac{2n_0P}{MNA} + \frac{n_0\lambda_{\text{exc}}}{NA^2}\exp\left(-\frac{2NAP}{M\lambda_{\text{exc}}}\right)\right\}$$

where n_0 is the refractive index of the object ($n_0 \sim 1.5$) and P the diameter of the confocal pinhole imaged on the object plane of the microscope ($P = 4\lambda$ in the present case). λ_{exc} and λ_{em} are wavelength of excitation and that of emitted fluorescence light, respectively. $\lambda_{\text{exc}} = \lambda_{\text{em}}$ for the reflection LSCM. M is the magnification of the objective. Using this equation, d_{axial} for our microscope ($\lambda = 0.488$ μm, $NA = 1.4$ M $= 100$) was calculated to be 0.53 μm.
(29) Wilhelm, S. About the 3D image quality of a confocal laser scanning microscope; Diploma Thesis, Fachhochschule; Köln, 1994.
(30) Ribbe, A. E.; Hashimoto, T.; Jinnai, H. *J. Mater. Sci.* **1996**, *31*, 5837.
(31) We have also performed reflection LSCM observations of a polymer blend of polystyrene (PS) and poly(vinylmethyl ether) (PVME) forming spherical domains of PS in the matrix of PVME. Again, only the interfacial region of the domains appeared bright and both the polystyrene and poly(vinyl methyl ether) domains were dark.
(32) Jinnai, H.; Nishikawa, Y.; Morimoto, H.; Koga, T.; Hashimoto, T. *Langmuir* **2000**, *16*, 4380.
(33) In Figure 3a, bright objects can also be found in the dark PB-rich domains. These structures might be formed by a small amount of SBR chains in the PB-rich domains.
(34) Although SBR/PB blends have been extensively studied and the size of the fine structure is relatively large, the existence of the fine structure has never been reported previously to our best knowledge. One of the reasons why the structure has not been recognized may be due to the difficulties in obtaining sufficient contrast under transmission electron microscopic (TEM) observations. The contrast generations in reflection LSCM and TEM are completely different. The contrast in reflection LSCM originates from the interfaces between the regions having different refractive indices or from difference in scattering power as in the case of our SBR/PB−AN samples. Generally speaking, LSCM is quite sensitive to the small differences in the refractive indices. On the other hand, the contrast of TEM depends on the differences in extinction cross section of electron beams between the two

phases. We have tried our best to observe the fine structure using TEM by staining the sample with OsO_4 to various degrees to find the best contrast between the styrene-segment-rich and butadiene-segment-rich phases. Although we could easily image the PB-rich and SBR-rich domains, the fine structure probed by reflection LSCM inside SBR-rich domains could not be ever detected. The weak selectivity of OsO_4 staining towards the small composition differences that might be due to the fine structures could be a reason. In other words, the fine structures appeared in the LSCM images are not well-defined structural entities.

(35) Tanaka, H *Phys. Rev. E* **1993**, *47*, 2946. Tao, J.; Okada, M.; Nose, T.; Chiba, T. *Polymer* **1995**, *36*, 3919. Hashimoto, T.; Hayashi, M.; Jinnai, H. *J. Chem. Phys.* **2000**, *112*, 6886. Hayashi, M.; Jinnai, H.; Hashimoto, T. *J. Chem. Phys.* **2000**, *112*, 6897. Hayashi, M.; Jinnai, H.; Hashimoto, T. *J. Chem. Phys.* **2000**, *113*, 3414.

(36) Tanaka, Y.; Sato, H.; Nakafutami, Y. *Polymer* **1981**, *22*, 1721.

(37) We have performed the ozonolysis of the SBR used for the experiments in chloroform solution to degrade the isoprene units of the polymer. The GPC measurement of the solution obtained, in which the styrene sequences of the SBR were dissolved, suggested the existence of styrene sequences of more than 30 units.

(38) Laurer, J. H.; Ashraf, A.; Smith, S. D.; Spontak, R. J. *Langmuir* **1997**, *13*, 3, 2250.

(39) Inoue, S In *Video Microscopy*; Plenum: New York, 1986.

MA010190D